Nonlinear surface heating of a plane sample and modes of current transfer to hot arc cathodes

M. S. Benilov
Departamento de Física, Universidade da Madeira, Largo do Município, 9000 Funchal, Portugal
(Received 20 May 1998)

A hypothesis is suggested that nonuniqueness of multidimensional thermal balance of a finite sample heated by a nonlinear external energy flux may be a reason for the existence of multiple modes of current transfer to hot arc cathodes. In order to check this hypothesis, bifurcation analysis has been carried out of the equation of heat conduction in the body of a thermionic cathode supplemented with a boundary condition describing heating by the adjacent plasma. Multiple solutions have been found, one of them describing a diffuse mode and others describing various spot modes. Solutions describing spot modes have been calculated in the vicinity of bifurcation points and analyzed qualitatively outside this vicinity. Qualitative conclusions concerning a transition between the diffuse discharge and the first spot mode conform to available experimental information. [S1063-651X(98)00711-9]

PACS number(s): 52.40.Hf, 52.80.Mg

I. INTRODUCTION

The problem of multidimensional steady-state temperature distributions created in a plane sample by a nonlinear external heating was formulated and analyzed in [1] as a mathematical example exhibiting characteristic features of constricted current transfer from a plasma to an electrode. It was found that the problem has, under certain conditions, multiple solutions, which have been associated with different modes of current transfer to an electrode. The approach based on the bifurcation theory was used. It was shown that the bifurcation analysis provides valuable qualitative information on modes with current constriction, as well as an initial approximation for numerical calculations. In [2], the bifurcation analysis has been employed in order to study the effect of normal current density on cold glow cathodes. In [3], the theory originally developed in [1] was recast, for a two-dimensional case, into a somewhat different form; a particular case of the step-function dependence of the external heat flux on the surface temperature was considered.

Solutions found in [1] reveal some features typical for near-electrode current constriction in general, such as the effect of normal current density, which is observed on cold cathodes in glow discharges. On the other hand, a problem of a high technological interest exists in which the model of nonlinear external heating of a plane sample may not only represent a mathematical example, but also be physically adequate: This is the problem of multiple modes of current transfer to hot arc cathodes. The essence of the problem is as follows: current transfer to hot arc cathodes may occur in a spot mode, when nearly all the current is localized in a region occupying only a small fraction of the cathode surface (the spot), and in a diffuse mode, when the current is distributed over the front surface of the cathode in a more or less uniform way. A transition between the diffuse and spot modes is accompanied by hysteresis (see, e.g., [4]), i.e., a current range exists in which both a diffuse mode and a spot mode may occur, depending on the prehistory. Descriptions of experimental observations of multiple modes of current transfer to hot cathodes in high-pressure arcs can be found, e.g., in [5]; we mention also Ref. [6] as an example of a recent work. The question of multiple modes of current transfer to hot arc cathodes is of crucial importance, in particular, for high-pressure discharge lamps [7]. Note that diffuse and spot modes occur also at arc anodes (see, e.g., [8–10]); however, the question of anodes is beyond the scope of the present work.

In [7], equations describing the near-cathode plasma were solved jointly with an equation of electron emission from the cathode surface. Two solutions have been found for each surface temperature and near-cathode voltage drop, one of them with low values of the current density and the electric field at the cathode surface and another with high values. The cathode operates via Schottky-amplified thermionic emission in the framework of the first solution and via thermofield or field emission in the framework of the second solution. The first solution has been identified with the diffuse mode and the second one with the spot mode.

Similar physics has been discussed in [11]: The cathode operates via Schottky-amplified thermionic emission in one mode and in a regime close to pure field emission in another mode. The ion current makes up a reasonable fraction of the total current in the first mode and is negligible in the second mode, which resembles the concept of the diffuse and spot modes developed in the early work [12].

Note, however, that an adequate theoretical description of multiple modes of current transfer to a hot arc cathode does not necessarily involve essentially different physical mechanisms. This is rather a mathematical question of finding nonunique solutions: An adequate theoretical model of current transfer to hot arc cathodes must in some cases allow different steady-state solutions to exist for the same conditions, which describe different modes of current transfer.

A simple theoretical model of current transfer to hot arc cathodes (see, e.g., [5] and references therein) is based on the equation of heat conduction in the cathode body supplemented with a boundary condition $\kappa \partial T/\partial n = q(T,U)$ at the current-collecting surface, where κ is the thermal conductivity of the substance of the cathode, T is the temperature, n is a direction locally orthogonal to the surface and directed outside the cathode, $q(T,U)$ is the density of the heat flux from the plasma to the surface, and U is the near-cathode voltage

drop that is assumed to be the same for all points of the current-collecting surface and should be chosen in such a way that the integral current to the cathode surface take a prescribed value. The function $q=q(T,U)$ is calculated by means of analysis of a plasma layer adjacent to the cathode surface and is considered as known while treating the problem of heat conduction in the cathode body. According to the above, an adequate theoretical description of multiple modes of current transfer to hot arc cathodes amounts to finding nonunique solutions of this problem, i.e., to finding different temperature distributions inside the cathode and on its surface that may occur for the same conditions. It should be expected that one of these distributions will correspond to the diffuse mode and others will correspond to spot modes.

It is of interest to consider from this point of view the above-mentioned works [7,11]. It follows from [7] that plasma states in front of the cathode with a given temperature of the surface and a given voltage drop across the near-cathode region may be nonunique. Hence the function $q(T,U)$ may be multivalued. This may be a reason for nonuniqueness of temperature distributions in the cathode, i.e., one may think of solutions with different branches of the function $q(T,U)$. However, the question of whether these nonunique solutions describe spot modes requires a multidimensional solution of the heat conduction equation in the cathode body, which has not been attempted in [7]. In [11], the heat conduction equation in the cathode body has been solved numerically in the approximation of axial symmetry. However, no multiple solutions have been presented. A question remains open whether the solution [11] describes one mode that changes its appearance with a change of conditions or the solution under changing conditions passes through a bifurcation point in which it continuously switches from one mode to another.

With regard to multiple solutions to the above-described problem, the work [13] should be referred to in which the heat conduction equation in a cylindrical thermionic cathode was solved numerically in the approximation of axial symmetry. A unique solution has been found for a cathode geometry modeling experimental conditions; however two solutions have been found in a certain current range for a wide cathode (of a diameter equal to its height), one of them with a relatively uniform temperature distribution over the cathode surface (the diffuse mode) and another with a high temperature in the center of the cathode and a relatively cold periphery (the spot mode). A reason for existence of multiple solutions was not discussed.

Summarizing the above, one can say that a possible reason for the multiplicity of modes of current transfer to hot arc cathodes found in the literature is a multivalued character of the function $q(T,U)$. On the other hand, the mathematical treatment [1] indicates that another reason is possible: A multidimensional thermal balance of a finite sample heated by a nonlinear external energy flux may be non-unique. In other words, the equation of heat transfer in the cathode body may have multiple solutions if considered in more than one dimension even if the function $q(T,U)$ is single valued.

It is of considerable interest in such a situation to apply the approach [1] to the conditions of a thermionic cathode with the aim of solving the question of nonuniqueness of its thermal balance and, if multiple solutions exist, of a qualitative study of multiple modes of current transfer to thermionic cathodes described by these solutions. This task is attempted in the present work with the use of a model of a plasma layer at a thermionic cathode described in [14]. Analysis of the possibility of multiple modes due to the multivalued character of the function $q(T,U)$ caused by the multiplicity of plasma states for given cathode surface temperature and near-cathode voltage drop is left beyond the scope of the present work (see a remark in Sec. IV A in this regard).

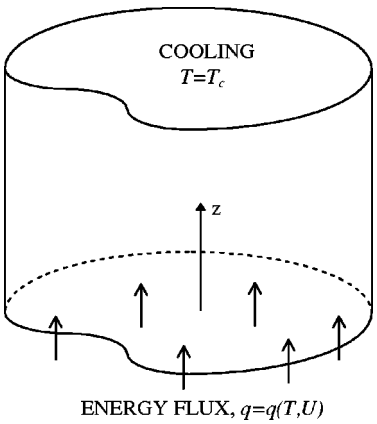

FIG. 1. Geometry of the problem.

A mathematical statement of the problem is given in Sec. II. General properties of solutions are discussed in Sec. III. In Sec. IV calculations are presented and discussed for conditions of thermionic cathodes. Concluding remarks are given in Sec. V.

II. MODEL

The model to be considered is illustrated by Fig. 1 and represents the above-mentioned model described in [5], applied to a particular case when a cathode is in the form of a right cylinder whose cross section is not necessarily circular, with the bottom surface being current collecting, the lateral (inactive) surface being thermally insulated, and the top being maintained at a fixed temperature T_c by external cooling. Joule heat production inside the cathode body is neglected. The density q of the heat flux to the current-collecting surface is considered as a given function of the local surface temperature T and of the voltage drop across the near-cathode layer U, which is constant along the current-collecting surface: $q=q(T,U)$. A steady-state temperature distribution within the cathode body is described by the nonlinear boundary-value problem

$$\nabla^2\psi=0, \tag{1}$$

$$\frac{\partial\psi}{\partial z}=-q(\psi,U) \quad \text{for } z=0,$$

$$\psi=0 \quad \text{for } z=h, \tag{2}$$

$$\frac{\partial\psi}{\partial n}=0 \quad \text{for } \Gamma.$$

Here the z axis is directed along the axis of the cylinder from the bottom inside the bulk of the cylinder, h is the height of

the cylinder, Γ designates the lateral surface, n is a direction orthogonal to the lateral surface in a point considered, and the function $\psi=\psi(T)$ is the heat flux potential related to the temperature by the equation

$$\psi(T)=\int_{T_c}^{T}\kappa(T)\,dT. \tag{3}$$

For brevity, ψ will be referred to as the temperature. It should be emphasized that if the density of the energy flux from the plasma is known as a function of T (and U), then it can be determined as a function of ψ; hence the function $q(\psi,U)$ on the right-hand side of the boundary condition at $z=0$ will be treated as given.

After the problem (1) and (2) has been solved for a given U and a distribution of the temperature over the bottom surface of the cathode has been found, one can determine a distribution of density j of the electric current coming to the cathode surface from the plasma, corresponding to this U. [It is implied that a dependence of j on the local temperature of the cathode surface and on the voltage drop in the near-cathode layer is known; this dependence is determined by means of analysis of the plasma layer adjacent to the cathode surface and is calculated simultaneously with the function $q(\psi,U)$.] The integral current I also may be determined. Finding a solution for various U, one can determine the current-voltage characteristic $U(I)$.

Before specifying particular forms of functions $q(\psi,U)$ and $j(\psi,U)$ (Sec. IV), we consider in Sec. III properties of solutions of the considered problem for functions of a general form. Certain conclusions that will be made in Sec. III depend on the signs of derivatives of these functions. Therefore, we discuss here briefly the signs to be expected for functions of physical interest.

If the voltage applied to the near-cathode layer increases while the temperature of the cathode surface remains constant, the density of the electric current coming to the cathode increases. The power jU deposited in the near-cathode layer also increases, which results in an increase of the energy flux to the cathode. Therefore, derivatives $\partial j/\partial U$ and $\partial q/\partial U$ will be assumed to be positive.

An increase of the temperature of the cathode surface improves conditions for current transfer, therefore the derivative $\partial j/\partial\psi$ will be assumed to be positive. The rate of energy losses from the cathode surface increases. However, the power deposited in the near-cathode layer at constant voltage increases as well, hence no conclusion on the sign of the derivative $\partial q/\partial\psi$ can be drawn.

If the temperature of the cathode surface increases at constant current density rather than at constant voltage, improvement of conditions of current transfer results in a decrease of U and, consequently, of the power deposited in the near-cathode layer. Thus the derivative $(\partial q/\partial\psi)_j$ taken at constant current density may be assumed to be negative.

III. GENERAL PROPERTIES OF SOLUTIONS

The problem (1) and (2) may have a one-dimensional (1D) solution $\psi=\psi(z)$ of the form

$$\psi=\left(1-\frac{z}{h}\right)\psi_w, \tag{4}$$

where $\psi_w=\psi_w(U)$ is a root of the transcendental equation

$$\frac{\psi_w}{h}=q(\psi_w,U). \tag{5}$$

The temperature at all points of the cathode surface is the same (and equal to ψ_w), hence this solution describes a diffuse mode of current transfer to the cathode.

Let us calculate the slope of the current-voltage characteristic $U(j)$ described by the 1D solution. Differentiating Eq. (5) with respect to U and resolving the obtained equation, one finds

$$\frac{d\psi_w(U)}{dU}=-\frac{h\dfrac{\partial q}{\partial U}}{h\dfrac{\partial q}{\partial\psi}-1}. \tag{6}$$

The derivative of the function $j[\psi_w(U),U]$ is

$$\frac{dj[\psi_w(U),U]}{dU}=\frac{\partial j}{\partial\psi}\frac{d\psi_w(U)}{dU}+\frac{\partial j}{\partial U}. \tag{7}$$

Substituting for $d\psi_w(U)/dU$ Eq. (6), one obtains the following expression for the slope of the current-voltage characteristic $U(j)$ described by the 1D solution:

$$\frac{dU}{dj}=-\frac{h\dfrac{\partial q}{\partial\psi}-1}{h\left(\dfrac{\partial q}{\partial U}\dfrac{\partial j}{\partial\psi}-\dfrac{\partial q}{\partial\psi}\dfrac{\partial j}{\partial U}\right)+\dfrac{\partial j}{\partial U}}. \tag{8}$$

Introducing the derivative $(\partial q/\partial\psi)_j$ taken at constant current density, one can rewrite Eq. (8) as

$$\frac{dU}{dj}=-\frac{h\dfrac{\partial q}{\partial\psi}-1}{\dfrac{\partial j}{\partial U}\left[1-h\left(\dfrac{\partial q}{\partial\psi}\right)_j\right]}. \tag{9}$$

Multiplying Eqs. (6) and (9), one finds

$$\frac{d\psi_w}{dj}=\frac{h\dfrac{\partial q}{\partial U}}{\dfrac{\partial j}{\partial U}\left[1-h\left(\dfrac{\partial q}{\partial\psi}\right)_j\right]}. \tag{10}$$

According to what has been said at the end of Sec. II, derivatives $\partial j/\partial U$ and $\partial q/\partial U$ are positive while $(\partial q/\partial\psi)_j$ is negative. It follows that the denominator of the right-hand side of Eq. (9) is positive. Hence the current-voltage characteristic of the diffuse discharge has extrema at points at which $h(\partial q/\partial\psi)[\psi_w(U),U]=1$, is growing at points at which $h(\partial q/\partial\psi)[\psi_w(U),U]<1$, and is falling at points at which $h(\partial q/\partial\psi)[\psi_w(U),U]>1$. The right-hand side of Eq. (10) is positive. Hence the temperature of the cathode surface

in the diffuse mode monotonically increases with an increase of current, without regard to whether U is growing or decreasing.

The second derivative of the current-voltage characteristic in an extreme point can be found to be

$$\frac{d^2U}{dj^2} = -\frac{h^2\dfrac{\partial q}{\partial U}}{\left(\dfrac{\partial j}{\partial U}\right)^2\left[1-h\left(\dfrac{\partial q}{\partial \psi}\right)_j\right]^2}\frac{\partial^2 q}{\partial \psi^2}. \tag{11}$$

It follows that an extremum of the current-voltage characteristic of the diffuse discharge is a maximum if $(\partial^2 q/\partial\psi^2)[\psi_w(U),U]>0$ and a minimum if $(\partial^2 q/\partial\psi^2)[\psi_w(U),U]<0$.

In addition to the 1D solution, the problem may have multidimensional solutions $\psi=\psi(x,y,z)$ that branch off from (or join) the 1D solution. Bifurcation points in which branching or joining occur and solutions in the vicinity of these points may be found by means of a bifurcation theory given in the Appendix. In particular, a procedure of determination of the bifurcation points is as follows. Suppose that the 1D solution has been determined, i.e., Eq. (5) has been solved for all U of interest and the dependence $\psi_w=\psi_w(U)$ calculated. After that, one should solve at each U the equation

$$\frac{\partial q}{\partial \psi}[\psi_w(U),U] = k\coth kh, \tag{12}$$

thus determining a wave number k of steady-state perturbations that can branch off at the value of U considered. [Note that the function $k(U)$ does not depend on the cross section of the cathode.] After that, values of U should be identified at which the wave number $k(U)$ takes the values k_1, k_2, k_3, . . . determined by the spectrum of the Neumann problem (A9) for the two-dimensional Helmholtz equation considered in the cross section of the cathode. Just these will be the bifurcation points for a given cross section.

Since $x\coth x>1$ for real x, a necessary condition for Eq. (12) to have a real root is

$$h\frac{\partial q}{\partial \psi}[\psi_w(U),U]>1. \tag{13}$$

It follows from the above that this inequality is fulfilled on falling sections of a current-voltage characteristic $U(I)$ of the diffuse discharge. Thus, branching of multidimensional solutions from (as well as joining to) a 1D solution may occur only on a falling section of the current-voltage characteristic described by the 1D solution. Note that previously this conclusion has been derived [1] for the special case when the current density is related to the heat flux density by the formula $q(T,U)=U\,j(T,U)+\text{const}$.

Formulas describing the asymptotic behavior of multidimensional solutions in the vicinity of bifurcation points are given in the Appendix. Also given are formulas describing current-voltage characteristics of multidimensional solutions in the vicinity of bifurcation points. It follows from Eq. (A22) that the current-voltage characteristic of a multidimensional solution branches off into the region to the right of (or, equivalenty, above) the current-voltage characteristic of the diffuse discharge if the quantity

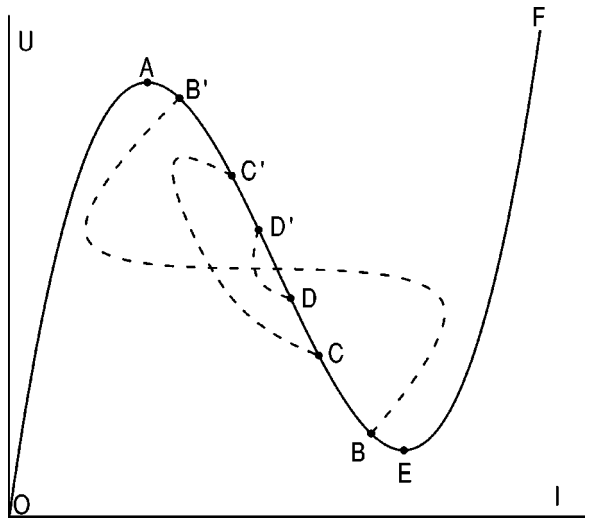

FIG. 2. Prototypical current-voltage characteristics. Solid line, diffuse mode; dashed lines, spot modes; A and E, extreme points of the current-voltage characteristic of the diffuse mode; B and B', bifurcation points associated with the first positive eigenvalue k_1; C and C', bifurcation points associated with k_2; D and D', bifurcation points associated with k_3.

$$\frac{\partial^2 j}{\partial \psi^2} - C_1 h\frac{\partial j}{\partial \psi}\frac{\partial^2 q}{\partial \psi^2} \tag{14}$$

evaluated at the bifurcation point is positive. [Here and below C_1 is a (positive) coefficient defined by Eq. (A12) or, equivalenty, by the equation $C_1=(h\,\partial q/\partial\psi-1)^{-1}$.] If the quantity (14) is negative, the current-voltage characteristic of a multidimensional solution branches off into the region to the left of (below) the current-voltage characteristic of the diffuse discharge.

In the vicinity of an extreme point of the current-voltage characteristic of the diffuse discharge, the quantity C_1 is large and the second term of expression (14) is dominating. According to what has been said at the end of Sec. II, the derivative $\partial j/\partial\psi$ is positive. Taking into account the conclusion on the sign of the derivative $\partial^2 q/\partial\psi^2$ in an extreme point drawn above, one can deduce that if a multidimensional solution branches off in the vicinity of the point of minimum or maximum, then the characteristic described by this solution branches off into the region above or, respectively, below the characteristic of the diffuse discharge.

We consider as a prototypical current-voltage characteristic of a diffuse discharge the one depicted in Fig. 2, which contains two sections of growth (sections OA and EF) separated by a falling section (AE). The quantity $h\,\partial q/\partial\psi$ on the section AE first grows from unity to a maximum value and then decreases back to unity. The wave number, being related to $\partial q/\partial\psi$ by Eq. (12), on the section AE first grows from zero to a maximum value $k_{\max}$ and then decreases back to zero. Obviously, each value of k below $k_{\max}$ is encountered two times on the section AE. In such a case, two bifurcation points are associated with each positive eigenvalue $k_i<k_{\max}$.

It is natural to suppose that a multidimensional solution that branches off at one of these two points joins at the other one, as is shown by dashed lines in Fig. 2. This hypothesis was confirmed by numerical calculations [1].

If the height of the cylinder is not too large compared to its transversal dimensions, then bifurcation points associated with the first positive eigenvalue k_1 are positioned not far away from extrema of the current-voltage characteristic of the diffuse discharge. According to the above, characteristic BB' in such a situation branches off at the point B from the characteristic of the diffuse discharge above and rejoins the characteristic of the diffuse discharge at the point B' from below, as is shown in Fig. 2.

The behavior of multidimensional solutions in a special case when the height of the cylinder is much smaller than its transversal dimensions is described by analysis [15]. Bifurcation points associated with eigenvalues with finite numbers are positioned in the vicinity of extrema of the current-voltage characteristic of the diffuse discharge. A schematic of the current-voltage characteristic for this case is represented by the dashed line BB' in Fig. 2. The current-voltage characteristic reveals a plateau, i.e., the effect of normal current density takes place in this case. The normal voltage U_n, i.e., a value of the near-cathode voltage that corresponds to the plateau, is determined by the condition

$$\int_{\psi_1}^{\psi_3} q(\psi, U_n)\, d\psi = \frac{1}{2h}(\psi_3^2 - \psi_1^2), \tag{15}$$

where ψ_1 and ψ_3 are values of the surface temperature that occur at $U = U_n$ on the sections OA and EF, respectively, of the current-voltage characteristic of a diffuse discharge. This equation may be derived by means of writing Eq. (1) in the vicinity of the boundary of the spot in two dimensions z, λ, where λ is the along-surface coordinate normal to the boundary, and then either by transforming this equation to an integral equation [3] or by multiplying it by a derivative $\partial\psi/\partial\lambda$ and integrating in λ and z [15].

IV. MODELING OF CURRENT TRANSFER TO HOT ARC CATHODES

A. Function $q = q(T, U)$

A plasma layer adjacent to the cathode surface should be calculated in order to find the density of the energy flux from the plasma to the surface, $q = q(T, U)$. A model [14] of a plasma layer at a thermionic cathode was used in the present work. Calculations presented below were carried out for argon and mercury plasmas. The parameter α appearing in the model [14] was calculated in terms of the ionization coefficient given in [16] and the diffusion coefficient of ions in the atom gas was calculated by means of cross sections [17,16] for the argon and mercury plasmas, respectively.

The calculation of the near-cathode plasma layer is reduced to solving a transcendental equation for the electron temperature in the framework of the model [14]. Two roots of this equation have been detected in some cases, a bigger root being of the order of 10^5 K. We discarded this root, thus leaving beyond the scope of the present work the question of whether this root corresponds to a physically possible state of the near-cathode plasma or it is physically irrelevant, having appeared due to the inapplicability of the model [14] at electron temperatures that high.

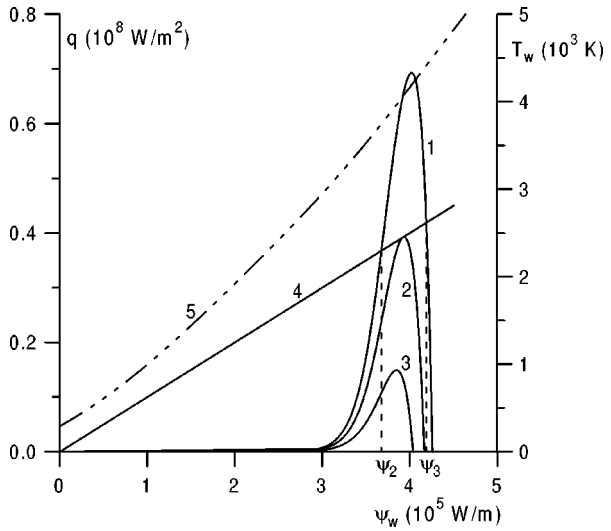

FIG. 3. Graphic illustration of the 1D heat balance of a tungsten cathode of a height of 10 mm in the atmospheric-pressure argon plasma. 1–3, the function $q = q(\psi_w, U)$ for $U = 12$, 11.13, and 10 V, respectively; 4, $q = \psi_w / h$; 5, the dependence $T_w(\psi_w)$ for tungsten.

The mechanism of electron emission in the model [14] is Schottky-amplified thermionic emission. Secondary electron emission (the γ process) is neglected, which is a usual approximation of the theory of thermionic cathodes; see, e.g., the discussion in [5]. Hence the results of the present work become inapplicable in the case of a cold cathode with a near-cathode voltage of the order of several hundred volts, when a contribution of the secondary electron emission to the total electron emission current becomes significant.

B. Diffuse mode

One needs to solve Eq. (5) in order to find a 1D solution associated with the diffuse mode of current transfer. As an example, graphs of the right-hand side of Eq. (5) for a tungsten cathode in the atmospheric-pressure argon plasma for three values of the voltage drop in the near-cathode layer are shown in Fig. 3 by curves 1–3. The straight line represents the left-hand side of Eq. (5) for a cathode of a height of 10 mm. For convenience, the relationship between the temperature and the heat flux potential of tungsten is also shown.

One can see that if $U \gtrsim 11.13$ V, Eq. (5) has two positive roots (designated by ψ_2 and ψ_3). As U decreases, the smaller root ψ_2 increases and the bigger one ψ_3 decreases. The roots merge at U approximately equal to 11.13 V. No positive roots exist if $U \lesssim 11.13$ V.

The voltage drop in the near-cathode layer and the temperature of the cathode surface as functions of the current density for a tungsten cathode of height $h = 10$ mm in the atmospheric-pressure argon plasma are represented in Fig. 4. The roots ψ_2 and ψ_3 are associated with the falling and growing sections AE and EF, respectively, of the curve $U(j)$.

It is of interest to discuss a connection between curve 1 representing the dependence $U(j)$ in Fig. 4 and the solid line representing the current-voltage characteristic of the diffuse

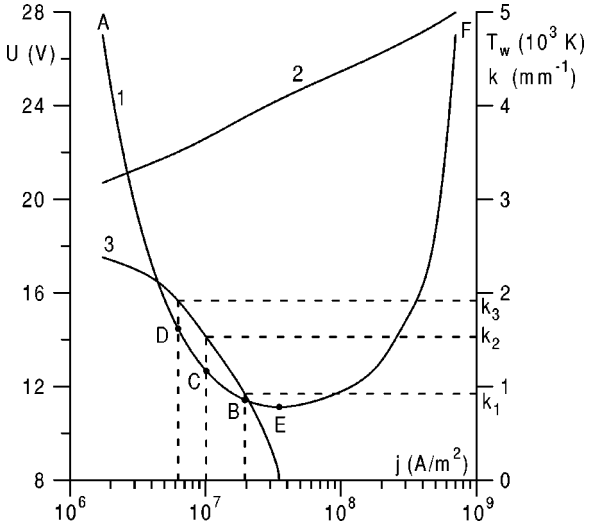

FIG. 4. Voltage drop in the near-cathode layer, temperature of the cathode surface, and wave number for the diffuse discharge on a tungsten cathode of a height of 10 mm in the atmospheric-pressure argon plasma. 1, the voltage drop; 2, the temperature of the cathode surface; 3, the wave number; *B*, *C*, and *D*, bifurcation points associated with the eigenvalues k_1, k_2, and k_3, respectively, for the case of a cathode in the form of a circular cylinder of a radius of 2 mm; *E*, the point of minimum of the voltage drop.

discharge in Fig. 2. Note that Eq. (5), apart from positive roots, has also a trivial root $\psi_w=0$ that exists for all U. This root corresponds to the situation in which no current flows to the cathode, $j=0$. Thus a current-voltage characteristic on the whole includes not only the branch represented in Fig. 4 by the curve 1, but also a branch coinciding with the axis of voltages. While the first branch exists for U exceeding approximately 11.13 V (the power supply is insufficient to heat up the whole surface of the cathode at lower voltages), the second branch exists for all voltages.

One can see that the current-voltage characteristic of a diffuse discharge on a thermionic cathode is of the type depicted in Fig. 2, however, with an important difference: The section *OA* coincides with the axis of voltages and the point *A* is at infinity in the conditions of a thermionic cathode. Obviously, this difference results from the fact that the function $q(T_w,U)$ in the model of a thermionic cathode tends to zero as $T_w \to T_c$.

Figure 3 supplies a graphic illustration of the relation between the slope of the current-voltage characteristic of the diffuse discharge and the local value of the quantity $h\,\partial q/\partial\psi$, discussed in Sec. III: The slope of curve 1 at the point $\psi=\psi_2$, which belongs to the falling section of the current-voltage characteristic, is larger than the slope of the straight line 4, which means that $\partial q/\partial\psi > 1/h$ at this point; the slope of curve 1 at the point $\psi=\psi_3$, which belongs to the growing section, is smaller than the slope of the straight line 4, which means that $\partial q/\partial\psi < 1/h$ at this point; the slopes of curve 2 and the straight line 4 at the tangent point are equal, which means $\partial q/\partial\psi = 1/h$ at the point of minimum of the current-voltage characteristic. One can see from Fig. 4 that the temperature of the cathode surface monotonically increases with an increase of the current density, which conforms to the general reasoning of Sec. III.

C. Normal voltage

One needs to solve Eq. (15) in order to find the normal voltage. Since the section *OA* of the current-voltage characteristic of the diffuse discharge in Fig. 2 coincides with the axis of voltages in the conditions of a thermionic cathode, one should set $\psi_1=0$ in Eq. (15) while treating a thermionic cathode. A geometrical sense of this equation may be illustrated as follows: If one considers a half strip $\{0 \leqslant \psi_w \leqslant \psi_3,\ q \geqslant 0\}$ in the plane (ψ_w, q) (Fig. 3), then areas of the half strip under the curve $q=q(\psi_w,U_n)$ and under the straight line $q=\psi_w/h$ are equal. This equation may be interpreted as a condition of the coexistence of phases, one phase being a normal spot and another being a surrounding discharge-free region, and may be called Maxwell's construction for a normal spot on a thermionic cathode.

Calculations for a tungsten cathode of the height of 10 mm in the atmospheric-pressure argon plasma give $U_n \approx 13.56$ V.

D. Bifurcation analysis

The procedure of finding bifurcation points is described in Sec. III. All bifurcation points are positioned on the falling section *AE* of the current-voltage characteristic of a diffuse discharge on a thermionic cathode shown in Fig. 4, as they do in the situation depicted in Fig. 2. Before proceeding to the results of calculations, we consider a question of whether the bifurcation points should be expected to exist in pairs in the case of a thermionic cathode, as they do in the situation depicted in Fig. 2.

The reasoning of Sec. III that leads to the conclusion that bifurcation points exist in pairs under the conditions of Fig. 2 is based on the fact that the current-voltage characteristic in Fig. 2 has two extreme points (a maximum and a minimum), in contrast to the current-voltage characteristic of a diffuse discharge on a thermionic cathode, which has only a minimum point. However, the presence of two extreme points on a current-voltage characteristic of a diffuse discharge is not a necessary condition for bifurcation points to exist in pairs, which can be seen from the following mathematical example. Consider a case when the function $q(\psi,U)$ is similar to that shown in Fig. 3, while its asymptotic expansion at $\psi \to 0$ is

$$q(\psi,U) = q_* \frac{\psi}{\psi_*}\left(\ln\frac{\psi_*}{\psi}\right)^{-1} + \cdots. \tag{16}$$

Here and in the following q_* is an infinitely growing function of U and ψ_* is a fixed parameter. Substituting the first term of the expansion (16) into Eq. (5), one gets an equation with two roots: a trivial one $\psi_w=0$, which belongs to the branch of the current-voltage characteristic of the diffuse discharge that coincides with the axis of voltages, and a positive root $\psi_w=\psi_*\exp(-q_*h/\psi_*)$, which belongs to the falling section of the current-voltage characteristic and tends to zero at large U. Differentiating the first term of the expansion (16) with respect to ψ and substituting the positive root, one finds that $h\,\partial q/\partial\psi$ on the falling section of the current-voltage characteristic tends to unity at large U. Thus the current-voltage characteristic of a diffuse discharge in this example is similar to that of the diffuse discharge on a ther-

mionic cathode, i.e., includes a branch coinciding with the axis of voltages and a branch with a minimum; however, the quantity $h\,\partial q/\partial\psi$ on the falling section is nonmonotonic and bifurcation points exist in pairs, as it is in the situation depicted in Fig. 2.

The considered mathematical example is representative for a glow discharge on a cold cathode: The current-voltage characteristic of a diffuse glow discharge includes a branch coinciding with the axis of voltages and a branch with a minimum, while bifurcation points on the falling section of the current-voltage characteristic exist in pairs [2]. As far as a thermionic cathode is concerned, one can see from Fig. 3 that the function $q(\psi,U)$ decreases with a decrease of ψ much faster than it is described by Eq. (16). In order to obtain a more adequate example, one can replace the first term on the right-hand side of the expansion (16) by the Arrhenius function

$$q(\psi,U)=q_*\exp\left(-\frac{\psi_*}{\psi}\right)+\cdots. \tag{17}$$

For this example, the quantity $h\,\partial q/\partial\psi$ on the falling section of the current-voltage characteristic of the diffuse discharge infinitely increases at large U [proportionally to $\ln(q_*h/\psi_*)$]. Thus there are no reasons to expect a nonmonotonic behavior of $h\partial q/\partial\psi$ on the falling section of the current-voltage characteristic and the presence of more than one bifurcation point per eigenvalue under the conditions of a thermionic cathode.

The results of numerical calculations conform to this conclusion: The quantity $h\partial q/\partial\psi$ on the falling section of the current-voltage characteristic of the diffuse discharge monotonically increases with an increase of U in all the cases considered, so multiple bifurcation points associated with a single eigenvalue have not been detected. As an example we determine bifurcation points for a tungsten cathode in the form of a circular cylinder of a height of 10 mm and of a radius R in the atmospheric-pressure argon plasma. The results of the calculation of the wave number are shown in Fig. 4. The first three positive eigenvalues of the Neumann problem for the two-dimensional Helmholtz equation in a circle are (see the Appendix)

$$k_1=1.841/R,\quad k_2=3.054/R,\quad k_3=3.832/R. \tag{18}$$

Bifurcation points associated with these eigenvalues are shown in Fig. 4 for $R=2$ mm. As it is pointed out above, only one bifurcation point was found for each eigenvalue. For clarity, the dashed lines have been added to Fig. 4 that illustrate finding bifurcation points after a distribution of the wave numbers along the current-voltage characteristic $k(j)$ and the spectrum $k,k_2,\ldots$ have been determined.

The asymptotic behavior of multidimensional solutions in the vicinity of bifurcation points follows from the results given in the Appendix. In particular, the distribution of the surface temperature is

$$\psi(x,y,0;U)=\psi_w(U_1)+4.094J_1\left(1.841\frac{r}{R}\right)\times\cos(\theta+\beta_1)\sqrt{C_9(U-U_1)}+\cdots, \tag{19}$$

$$\psi(x,y,0;U)=\psi_w(U_2)+5.439J_2\left(3.054\frac{r}{R}\right)\times\cos(2\theta+\beta_2)\sqrt{C_9(U-U_2)}+\cdots, \tag{20}$$

$$\psi(x,y,0;U)=\psi_w(U_3)-\left[C_1h\frac{\partial q}{\partial U}+5.677C_2J_0\left(3.832\frac{r}{R}\right)\right]\times(U-U_3)+\cdots, \tag{21}$$

where U_i is a value of the voltage drop that corresponds to the ith bifurcation point, r is the distance from the center of the circle, θ is the azimuthal angle, $J_\nu(z)$ are the Bessel functions, β_1 and β_2 are arbitrary angles, and the coefficients C_2 and C_9 are given by Eqs. (A16) and (A40), respectively.

A two-term asymptotic expansion of the function $\psi_w(U)$ in the vicinity of the point $U=U_i$ can be found by means of Eq. (6),

$$\psi_w(U)=\psi_w(U_i)-C_1h\frac{\partial q}{\partial U}(U-U_i)+\cdots. \tag{22}$$

It follows that the term $\psi_w(U_1)$ on the right-hand side of Eq. (19) as well as the term $\psi_w(U_2)$ on the right-hand side of Eq. (20) may be replaced, in the approximation being considered, by $\psi_w(U)$. Equation (21) can be rewritten as

$$\psi(x,y,0;U)=\psi_w(U)-5.677C_2J_0\left(3.832\frac{r}{R}\right)\times(U-U_3)+\cdots. \tag{23}$$

One can see from Eq. (19) that a one-parameter family of 3D solutions branches off at the first bifurcation point. If $C_9>0$, the solutions exist in the range $U\geqslant U_1$, i.e., are supercritical. If $C_9<0$, the solutions exist in the range $U\leqslant U_1$, i.e., are subcritical. Perturbations described by these solutions increase with increasing distance to the bifurcation point proportionally to $\sqrt{|U-U_1|}$. The function $J_1(k_1r)$ increases monotonically in the range $0\leqslant r\leqslant R$, hence the perturbations of the cathode surface temperature have a point of maximum somewhere at the ring $r=R$. Thus the solutions branching off at the first bifurcation point describe the beginning of the formation of a spot at the edge of the cathode. Since these solutions are identical to the accuracy of a rotation, they can be considered as a single solution with an arbitrary azimuthal position of the spot.

Similarly, 3D solutions branching off at the second bifurcation point can be considered as a single solution describing the beginning of the formation of a system of two spots positioned opposite each other at the edge of the cathode, with an arbitrary azimuthal orientation of the system. This solution is supercritical if $C_9>0$ and subcritical if $C_9<0$.

Calculations for $R=2$ mm indicate that C_9 is positive for both $i=1$ and $i=2$. Hence 3D solutions describing modes with a spot at the edge and two spots at the edge are supercritical in the conditions considered.

An axially symmetric solution that branches off at the third bifurcation point exists for U both below and above

U_3, i.e., has both sub- and supercritical branches. Perturbations described by this solution grow proportionally to $U-U_3$. $J_0(k_3 r)$ is monotonically decreasing in the range $0 \leqslant r \leqslant R$, hence the supercritical branch describes axisymmetric perturbations of the cathode surface temperature with a maximum either at the center or everywhere at the edge of the cathode (at the ring $r=R$), depending on whether C_2 is negative or positive. The subcritical branch describes perturbations with a maximum at the center if $C_2>0$ and at the edge if $C_2<0$. Thus the axisymmetric solution branching off at the third bifurcation point describes two physically different modes: a mode with a spot at the center of the cathode and a mode with a ring spot at the edge.

Calculations for $R=2$ mm indicate that C_2 is positive for $i=3$. Thus the supercritical branch describes the mode with a ring spot and the subcritical branch describes the mode with a spot at the center.

Current-voltage characteristics of the spot modes in the vicinity of a respective bifurcation point are described by Eq. (A42) for $i=1,2$ and by Eq. (A33) for $i=3$. One can see that the difference $\langle j \rangle - j_{1D}$ increases proportionally to $U-U_i$ for $i=1,2$ and to $(U-U_3)^2$ for $i=3$. Hence the current-voltage characteristics of modes with one or two spots at the edge branch off from the current-voltage characteristic of the diffuse mode at a certain angle; the characteristics of the modes with a spot at the center and a ring spot at the edge have the same slope at the bifurcation point as the characteristic of the diffuse mode. Calculations for $R=2$ mm indicate that the quantity (14) is positive at all three bifurcation points, hence current-voltage characteristics of the spot modes branch off into the region above the current-voltage characteristic of the diffuse mode.

The current-voltage characteristic of the diffuse discharge on a tungsten cathode of a height of 10 mm and radius of 2 mm in the atmospheric-pressure argon plasma in the variables I,U is shown in Fig. 5. Sections of the curves BB' and CC' depicted by solid lines represent the asymptotic behavior of characteristics of the modes with one and two spots at the edge, respectively. The characteristics of the modes a spot at the center and with a ring spot at the edge are indistinguishable in the vicinity of the bifurcation point D from the characteristic of the diffuse discharge, which is a consequence of the fact that terms of the quantity (14) at the point D nearly compensate for each other (the difference between these terms is about 10% of their sum).

The above analysis allows one to draw some qualitative conclusions concerning current-voltage characteristics of the spot modes outside the vicinity of bifurcation points. A trend that can be seen in Fig. 2 is that the current-voltage characteristics of spot modes, once having branched off at the points B, C, and D, go up; the characteristics CC' and DD' that branch off into the region between the growing section OA of the current-voltage characteristic of the diffuse mode and the falling section AE remain in this region; the characteristic BB' that branches off into the region between the falling section AE and the growing section EF turns back to AE, crosses it, and then remains in the region between OA and AE.

It is expected that this trend will remain the same also for the thermionic cathode considered here. On the other hand, the presence of no more than one bifurcation point per eigenvalue indicates that a solution with a spot, once having branched off from the 1D solution, will not rejoin the latter. In other words, the current-voltage characteristic of the modes with spots in Fig. 5 that branch off from the line AE at the points B, C, and D will not rejoin AE, in contrast to lines BB', CC', and DD' in Fig. 2. Thus a possible scenario is as follows: The characteristics, after having left the vicinity of bifurcation points, turn back to the falling section EA of the current-voltage characteristic of the diffuse mode, cross it, and then go up to infinity, being positioned between the section AE and the axis of voltages. This scenario is depicted in Fig. 5 by the dashed lines.

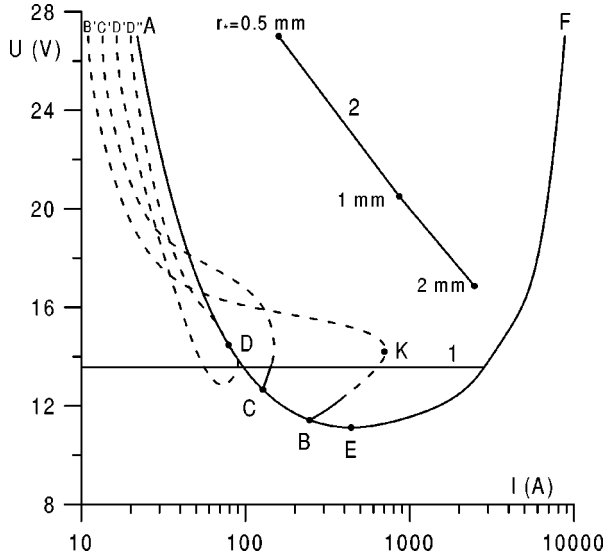

FIG. 5. Current-voltage characteristics of various modes of current transfer to a tungsten cathode of a height of 10 mm and radius of 2 mm in the atmospheric-pressure argon plasma. AEF, the diffuse mode; BB', the mode with a spot at the edge; CC', the mode with two spots at the edge; DD', the mode with a spot at the center; DD'', the mode with a ring spot at the edge; 1, the normal-spot mode; 2, the spot on an infinite plane cathode; E, the point of minimum of the current-voltage characteristic of the diffuse mode.

It is of interest to compare the above conclusions with the results of numerical calculations [13], carried out for a tungsten cathode in the form of a circular cylinder in the atmospheric-pressure argon plasma. A solution with a spot at the center of the cathode as well as that describing the diffuse mode have been found in [13] for the case $h=6$ mm, $R=3$ mm. The current-voltage characteristics of the two modes fit in the scenario shown in Fig. 5, which supports the qualitative considerations given above. On the other hand, the spot solution [13] does not join the solution describing the diffuse mode, which means that the former has been found only in a part of its existence region; the second axisymmetric spot mode discussed aboved (the one with a ring spot) was not found. This is a manifestation of a difficulty inherent to numerical methods in problems with multiple solutions: If the number of solutions is unknown, one cannot be sure that solution(s) found numerically represent the whole spectrum of existing solutions.

The data in Fig. 5 have been calculated for the cathode radius of 2 mm. With an increase of the radius, the current-voltage characteristic of the diffuse mode will shift to larger currents while the bifurcation points B, C, and D will move

closer to the point of minimum E. Characteristics of the spot modes will tend to show the normal current density effect, i.e., will reveal a plateau at $U=U_n$. (The plateau is shown in Fig. 5 by the horizontal line.) The characteristics of the mode with a spot in the center of the cathode and the mode with two spots at the edge will tend at high voltages closer to the current-voltage characteristic of a spot on an infinite plane cathode. (This characteristic was calculated by means of the model [14] with the changes described in Sec. IV A and is shown in Fig. 5 by line 2; the numbers near the line designate values of the spot radius.) The characteristic of the mode with a spot at the edge will tend at high voltages closer to the current-voltage characteristic of a spot on an infinite plane cathode displaced to lower currents by a factor of 2.

One can see from Fig. 5 that the diffuse mode is the only one possible at high currents. It is expected that the diffuse mode at constant current is unstable on a falling section of the current-voltage characteristic beyond the first bifurcation point, i.e., on the section BB' in Fig. 2 and on the section BA in Fig. 5. Hence a discharge that burns initially in the diffuse mode will switch to a spot mode when the current has been decreased down to the value I_B corresponding to the point B. (More accurately, I_B is a limit below which the diffuse discharge on a cathode with an ideally uniform surface becomes unstable against infinitely small perturbations; in fact, the switching may occur at somewhat higher currents due to surface nonuniformities and/or finite perturbations.) The question of which spot mode will occur requires a calculation of spot modes beyond the vicinity of bifurcation points and investigation of their stability; an occurrence of the first mode (the mode with a spot at the edge) seems likely.

Since the diffuse mode is unstable at small currents, the discharge at small currents can burn only in a spot mode. With an increase of current, a switching to the diffuse mode occurs. The question of a current value at which this happens is a question of stability. It seems likely, however, that stability will be lost at maximum currents attainable in the spot mode, i.e., in the vicinity of the turning point (point K in Fig. 5). Since the respective current exceeds I_B, the transition between the modes is accompanied by hysteresis. This transition is schematically illustrated in Fig. 6. Thus the present theory predicts, in agreement with the experiment (see, e.g., [4]), a spot mode at low currents and the diffuse mode at high currents, with a transition accompanied by hysteresis.

According to the theory, the transition from the diffuse mode to the spot mode is accompanied in the above-described conditions by an increase of the voltage drop in the near-cathode layer. In other conditions, this transition may be accompanied by a decrease of the voltage drop. The latter applies, for example, to the case $R=2$ mm, $h=25$ mm, in which the current-voltage characteristic of the first spot mode branches off into the region below the current-voltage characteristic of the diffuse discharge and to the right of the line $I=I_B$. It is of interest to note in this connection that the arc voltage in the transition from the diffuse mode to the spot mode in most cases increases by a few volts (see, e.g., [18] nd also other references cited in [5]). The arc voltage may be divided into a near-anode voltage drop, an arc column voltage, a voltage drop in the near-cathode expansion zone, and the voltage drop in the near-cathode layer. It is natural to

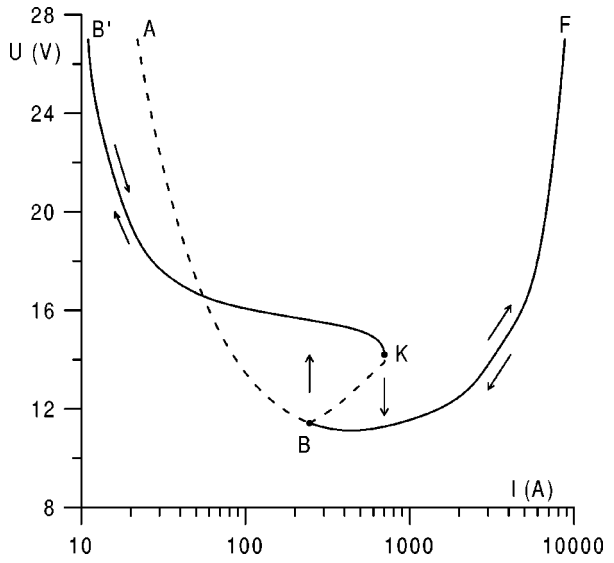

FIG. 6. Schematic of the transition between the diffuse mode and the mode with a spot at the edge on a tungsten cathode of a height of 10 mm and radius of 2 mm in the atmospheric-pressure argon plasma. ABF, the diffuse mode; $B'KB$, the mode with a spot at the edge; solid lines, sections of the current-voltage characteristics corresponding to stable states; dashed lines, sections corresponding to unstable states.

assume that the near-anode voltage drop and the arc column voltage are not affected by the change of a mode of current transfer at the cathode. If the voltage drop in the near-cathode expansion zone can be neglected, one will arrive at the conclusion that an increase of the arc voltage amounts to an increase of the voltage drop in the near-cathode layer. It is not clear, however, whether the voltage drop in the near-cathode layer can in fact be neglected: An order-of-magnitude estimate of this voltage drop may be obtained by multiplying the electric field in the arc column by the radius of the column; if one assumes the value of 10^3 V/m for the former and 1 mm for the latter the product will be 1 V, which is not really much smaller than the changes of the arc voltage measured. Thus the question of validity of the above reasoning requires further elaboration.

As it was pointed out above, the transition from the diffuse mode to the spot mode may be expected to occur in the framework of the present model at point B, i.e., at such a value j_B of the current density that the respective wave number $k(j_B)$ equals $k_1=1.841/R$. It is of interest to investigate the effect of control parameters on j_B and on the respective transition current I_B and to compare the information obtained with that given by the experiment.

The control parameters of the present model are the cathode radius, the cathode height, the cathode material, the plasma pressure, and species of the plasma-producing gas. The effect of the cathode radius can be seen from Fig. 4: j_B decreases with an increase of k_1, i.e., with a decrease of the cathode radius. I_B decreases even more strongly. It follows that a reduction of the front area of the cathode results in a decrease of the transition current, in accord with the experiment [5].

The effect of other control parameters is illustrated in Fig. 7, in which solid lines represent dependences $k(j)$ calculated for different conditions. Curve 1 has been calculated for the

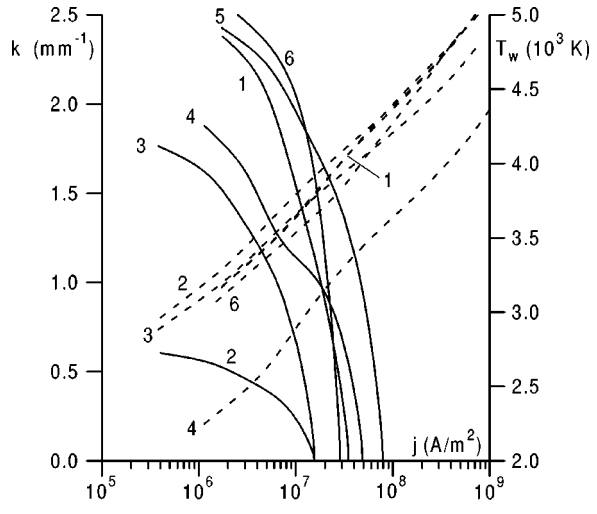

FIG. 7. Wave number (solid lines) and temperature of the cathode surface (dashed lines) for the diffuse discharge. 1, tungsten cathode of height $h=10$ mm in Ar plasma of pressure $p=1$ atm ; 2, $h=40$ mm; 3, zirconium cathode; 4, thoriated-tungsten cathode; 5, $p=5$ atm; 6, Hg plasma.

same variant as above and represents the same data that are shown in Fig. 4; all other variants differ from the that mentioned above by one of the parameters. Cathode materials have been chosen in order to illustrate separately the effects of the thermal conductivity and the work function, which are the parameters characterizing the cathode substance in the model [14]: Zirconium has an essentially lower thermal conductivity than tungsten and nearly the same work function, while thoriated tungsten has the same thermal conductivity and an essentially lower work function than (pure) tungsten. For convenience, the respective temperatures of the cathode surface and current-voltage characteristics are also presented (the dashed lines in Fig. 7 and the lines in Fig. 8). Note that

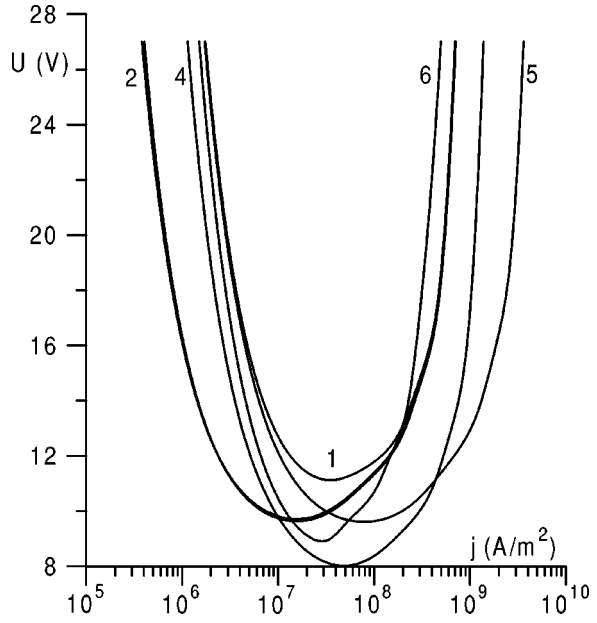

FIG. 8. Current-voltage characteristics of the near-cathode layer with a diffuse mode of current transfer. The parameters of the curves are the same as those in Fig. 7.

the dashed lines 1 and 5 in Fig. 7 coincide, as well as lines 2 and 3 in Fig. 8.

A comparison of variants 1 and 2 shows that a cathode design with an increased heat resistance results in a decrease of j_B, which conforms to the experiment [5]. A decrease of the thermal conductivity of the cathode material (variants 1 and 3) also results in a decrease of j_B, which again conforms to the experiment [5]. A decrease of the work function of the cathode material (variants 1 and 4) results in a small (up to 40%) increase of j_B for wide cathodes (of a radius exceeding approximately 2 mm) and a decrease of j_B for cathodes not too wide, the latter conclusion being in agreement with the experiment [19]. An increase of the argon pressure (variants 1 and 5) results in an increase of j_B. A substitution of an inert gas by mercury (variants 1 and 6) results in a small (up to 20%) decrease of j_B for wide cathodes (of a radius exceeding approximately 3 mm) and in an increase of j_B for cathodes not too wide, the latter conclusion being in agreement with the experiment [4].

One can conclude that, although a quantitative comparison of theoretical values of the transition current with available experimental data is not possible due to the idealized geometry of the cathode assumed in this work, a qualitative agreement is present.

V. CONCLUDING REMARKS

The equation of heat conduction has been considered in the body of a thermionic cathode in the form of a right cylinder. Bifurcation analysis shows that this equation, apart from a 1D solution describing a diffuse mode of current transfer to the cathode, has also multidimensional solutions describing various spot modes. Since these solutions have been obtained with the use of a single-valued function $q(T,U)$, it follows that the nonuniqueness of the multidimensional thermal balance of a finite sample heated by a nonlinear external energy flux may be the reason for the existence of multiple modes of current transfer to thermionic cathodes, in addition to or instead of the nonuniqueness of possible states of a plasma in the near-cathode layer for a given cathode surface temperature and a given voltage drop in the near-cathode layer.

One bifurcation point per eigenvalue has been found, in contrast to the case of a cold glow cathode when two bifurcation points are associated with an eigenvalue. It is of interest to emphasize that this contrast appears in spite of the similarity of the current-voltage characteristics of the diffuse mode, which in both cases includes a branch coinciding with the axis of voltages and a branch with a minimum. The presence of only one bifurcation point per eigenvalue indicates that a solution with a spot, once having branched off in this point from a 1D solution describing the diffuse mode, will not rejoin the latter. Qualitative conclusions have been drawn on current-voltage characteristics of modes with spots.

The results obtained qualitatively agree with available experimental information, thus supporting the hypothesis that the multiplicity of modes of current transfer to hot arc cathodes is related to the nonuniqueness of the multidimensional thermal balance of a cathode.

ACKNOWLEDGMENTS

The work has been performed within activities of the projects *Nonlinear, Stochastic and Complex Systems: Their Mathematical Theory and Application* of the program Praxis XXI (Portugal) and *Fundamental Characterization of Thermionic Cathodes* of BMBF (Germany) and was financially supported by FEDER and CITMA (Portugal) and by Heinrich-Hertz Stiftung (Germany). Part of the work has been carried out in Ruhr-Universität Bochum (Germany).

APPENDIX: BIFURCATION THEORY

Bifurcation analysis of the problem (1) and (2) is given in [1] for the case of nondegenerate eigenvalues. In this appendix results are presented for eigenvalues of arbitrary degree of degeneracy, which are needed, for example, to treat initial bifurcation points for a circular cylinder. Formulas are derived for current-voltage characteristics described by multidimensional solutions in the vicinity of bifurcation points. An application of the results obtained to the particular case of a circular cylinder is considered.

Suppose that $U=U_i$ is a bifurcation point and designate by $\psi_0(z)$ a respective 1D solution. We seek a solution in the vicinity of this point in the form of a series

$$\psi(x,y,z;U)=\psi_0(z)+\varepsilon\psi_1(x,y,z)+\frac{\varepsilon^2}{2}\psi_2(x,y,z)+\frac{\varepsilon^3}{6}\psi_3(x,y,z)+\cdots, \tag{A1}$$

where ε is a small parameter related to $U-U_i$. In order to incorporate cases of perturbations growing in the vicinity of the bifurcation point proportionally to $U-U_i$ or $\sqrt{|U-U_i|}$, we write

$$U=U_i+\varepsilon\alpha_1+\frac{\varepsilon^2}{2}\alpha_2 \tag{A2}$$

and will choose at a later stage either $\alpha_1=1$ and $\alpha_2=0$ or $\alpha_1=0$ and α_2 equal to 1 or -1, as it will be appropriate.

Problems governing the functions ψ_1,ψ_2,ψ_3 may be derived by differentiating Eqs. (1) and (2) with respect to ε once, twice, and three times, respectively, and setting $\varepsilon=0$:

$$\nabla^2\psi_p=0, \tag{A3}$$

$$-\frac{\partial\psi_p}{\partial z}-\frac{\partial q}{\partial\psi}\psi_p=F_p \quad \text{for } z=0,$$

$$\psi_p=0 \quad \text{for } z=h, \tag{A4}$$

$$\frac{\partial\psi_p}{\partial n}=0 \quad \text{for } \Gamma,$$

where the index p runs through values 1,2,3 and

$$F_1=\frac{\partial q}{\partial U}\alpha_1, \tag{A5}$$

$$F_2=\frac{\partial^2 q}{\partial\psi^2}\psi_1^2+2\frac{\partial^2 q}{\partial\psi\,\partial U}\psi_1\alpha_1+\frac{\partial^2 q}{\partial U^2}\alpha_1^2+\frac{\partial q}{\partial U}\alpha_2, \tag{A6}$$

$$F_3=\frac{\partial^3 q}{\partial\psi^3}\psi_1^3+3\frac{\partial^3 q}{\partial\psi^2\partial U}\psi_1^2\alpha_1+3\frac{\partial^3 q}{\partial\psi\,\partial U^2}\psi_1\alpha_1^2+\frac{\partial^3 q}{\partial U^3}\alpha_1^3+3\frac{\partial^2 q}{\partial\psi^2}\psi_1\psi_2+3\frac{\partial^2 q}{\partial\psi\,\partial U}(\psi_1\alpha_2+\psi_2\alpha_1)+3\frac{\partial^2 q}{\partial U^2}\alpha_1\alpha_2. \tag{A7}$$

Here and below all the derivatives of the function q are taken at $\psi=\psi(U_i)$, $U=U_i$, and the functions ψ_1 and ψ_2 on the right-hand sides of Eqs. (A6) and (A7) are evaluated at $z=0$.

Since a bifurcation occurs in the point considered, the problems (A3) and (A4) must have nonunique solutions. The respective homogeneous problem [which is obtained by dropping F_p on the right-hand side of the first boundary condition (A4)] must have a nontrivial solution. In other words, one should consider the homogeneous problem as an eigenvalue one, the role of the eigenvalue parameter being played by the quantity $\partial q/\partial\psi$, which is the only control parameter of the homogeneous problem for a given geometry.

Separating the variable z from x and y, one finds that the eigenvalues and the respective eigenfunctions of the homogeneous problem are related by the formulas

$$\frac{\partial q}{\partial\psi}=k_i\coth k_i h, \qquad \phi=\Phi(x,y)\sinh k_i(h-z) \tag{A8}$$

to the eigenvalues k_i and the eigenfunctions Φ of the Neumann problem for the two-dimensional Helmholtz equation

$$\frac{\partial^2\Phi}{\partial x^2}+\frac{\partial^2\Phi}{\partial y^2}+k_i^2\Phi=0 \quad \text{for } G,$$

$$\frac{\partial\Phi}{\partial n}=0 \quad \text{for } g, \tag{A9}$$

where G is the cross section of the cylinder, g is the boundary of the region G, and n is a direction locally orthogonal to g. It is known [20] that all eigenvalues of the problem (A9) are real and of finite degeneracy; a set of eigenvalues is countable and may be numbered in order of their increase, the eigenvalues growing unlimitedly with the increase of the number. We denote the set of eigenvalues numbered in order of their increase by $k_0,k_1,k_2,\ldots$. Let N_i $(i=0,1,2,\ldots)$ be a degeneracy of the ith eigenvalue and $\Phi_{im}=\Phi_{im}(x,y)$ $(i=0,1,2,\ldots;\ m=1,\ldots,N_i)$ be the orthonormal set of eigenfunctions ($\langle\Phi_{im}\Phi_{jk}\rangle=\delta_{ij}\delta_{mk}$, where the angular brackets designate averaging in x and y over the cross section of the cylinder). The second index will be dropped in the case of functions associated with nondegenerate eigenvalues. Note that $k_0=0$, $N_0=1$, $\Phi_0=1$, $k_i>0$, and $\langle\Phi_{im}\rangle=0$ for $i\geqslant 1$.

Multidimensional solutions branch off at bifurcation points associated with nontrivial k_i. Thus we assume that $i\geqslant 1$ in Eqs. (A8).

The inhomogeneous problems (A3) and (A4) are solvable provided that the inhomogeneous terms are orthogonal to the nontrivial solutions of the homogeneous problem

$$\langle F_p \Phi_{im} \rangle = 0 \tag{A10}$$

for each $m=1,\ldots,N_i$ and $p=1,2,3$. A solution may be found by means of expansion in eigenfunctions of the homogeneous problem and reads

$$\psi_p = -C_1 \langle F_p \rangle (h-z) + \sinh k_i (h-z) \sum_{m=1}^{N_i} A_m^{(p)} \Phi_{im} + \sum_{\substack{l=1 \\ l \neq i}}^{\infty} \sum_{m=1}^{N_l} \frac{\langle \Phi_{lm} F_p \rangle}{k_l \cosh k_l h - k_i \coth k_i h \sinh k_l h} \times \sinh k_l (h-z)\, \Phi_{lm}, \tag{A11}$$

where $A_m^{(p)}$ are arbitrary constants and

$$C_1 = (k_i h \coth k_i h - 1)^{-1}. \tag{A12}$$

It can be seen from Eq. (A11) that

$$\langle \psi_p(x,y,0) \rangle = -C_1 \langle F_p \rangle h. \tag{A13}$$

For $p=1$, the solvability condition (A10) is obviously satisfied (note that $F_1 = \text{const}$). The terms of the double sum on the right-hand side of Eq. (A11) vanish and one gets

$$\psi_1 = -C_1 \frac{\partial q}{\partial U} \alpha_1 (h-z) + \sinh k_i (h-z) \sum_{m=1}^{N_i} A_m^{(1)} \Phi_{im}. \tag{A14}$$

Analysis of the first approximation has been completed; however, coefficients $A_m^{(1)}$ remain indeterminate. The solvability condition of the equation of the second approximation should be considered in order to find these coefficients. The function F_2 may be found by substitution of Eq. (A14) into the right-hand side of Eq. (A6)

$$F_2 = \frac{\partial^2 q}{\partial \psi^2} \left(C_1 h \frac{\partial q}{\partial U} \alpha_1 \right)^2 - 2 C_1 h \frac{\partial^2 q}{\partial \psi\, \partial U} \frac{\partial q}{\partial U} \alpha_1^2 + \frac{\partial^2 q}{\partial U^2} \alpha_1^2 + \frac{\partial q}{\partial U} \alpha_2 + 2 \sinh k_i h\, C_2 \frac{\partial^2 q}{\partial \psi^2} \alpha_1 \sum_{m=1}^{N_i} A_m^{(1)} \Phi_{im} + \sinh^2 k_i h \frac{\partial^2 q}{\partial \psi^2} \sum_{m=1}^{N_i} \sum_{n=1}^{N_i} A_m^{(1)} A_n^{(1)} \Phi_{im} \Phi_{in}, \tag{A15}$$

where

$$C_2 = \frac{\partial^2 q}{\partial \psi\, \partial U} \left(\frac{\partial^2 q}{\partial \psi^2} \right)^{-1} - C_1 h \frac{\partial q}{\partial U}. \tag{A16}$$

Substituting Eq. (A15) into Eq. (A10) for $p=2$, one arrives at the following system of algebraic equations for coefficients $A_m^{(1)}$:

$$\frac{2 C_2 \alpha_1}{\sinh k_i h} A_v^{(1)} + \sum_{j=1}^{N_i} \sum_{m=1}^{N_i} \langle \Phi_{ij} \Phi_{im} \Phi_{iv} \rangle A_j^{(1)} A_m^{(1)} = 0, \tag{A17}$$

where $v=1,\ldots,N_i$.

In a general case, the system of equations (A17) has a trivial solution $A_m^{(1)}=0$, which corresponds to the 1D solution of the original problem (1) and (2), and solution(s) proportional to α_1, which correspond to multidimensional solution(s) branching off from the 1D solution. One can set $\alpha_1 = 1$ and $\alpha_2 = 0$ in this case, thus $\varepsilon = U - U_i$. Perturbations branching off at the considered bifurcation point grow proportionally to $U - U_i$.

Consider now a special case of a bifurcation point for which $\langle \Phi_{ij} \Phi_{im} \Phi_{iv} \rangle = 0$ for all j,m,v from 1 to N_i. In such a case, one should set $\alpha_1 = 0$ in order that Eq. (A17) allow nontrivial $A_m^{(1)}$. Thus the condition of solvability of the equation of the second approximation does not allow one to determine $A_m^{(1)}$ and one should consider the condition of solvability of the equation of the third approximation.

The function ψ_2 may be found by substituting Eq. (A15) into the right-hand side of Eq. (A11) for $p=2$

$$\psi_2 = -C_1 \left(\frac{\partial q}{\partial U} \alpha_2 + \sinh^2 k_i h \frac{\partial^2 q}{\partial \psi^2} \sum_{m=1}^{N_i} A_m^{(1)2} \right) (h-z) + \sinh k_i (h-z) \sum_{m=1}^{N_i} A_m^{(2)} \Phi_{im} + \sinh^2 k_i h \frac{\partial^2 q}{\partial \psi^2} \times \sum_{\substack{l=1 \\ l \neq i}}^{\infty} \sum_{m=1}^{N_l} \frac{\sum_{j=1}^{N_i} \sum_{n=1}^{N_i} A_j^{(1)} A_n^{(1)} \langle \Phi_{ij} \Phi_{in} \Phi_{lm} \rangle}{k_l \cosh k_l h - k_i \coth k_i h \sinh k_l h} \times \sinh k_l (h-z)\, \Phi_{lm}. \tag{A18}$$

Using this expression for evaluation of F_3 and substituting the result into the right-hand side of Eq. (A10) for $p=3$, one obtains the following system of algebraic equations for coefficients $A_m^{(1)}$:

$$\frac{3 C_2 \alpha_2}{\sinh^2 k_i h} A_v^{(1)} + \sum_{j=1}^{N_i} \sum_{m=1}^{N_i} \sum_{n=1}^{N_i} \left[\frac{\partial^3 q}{\partial \psi^3} \left(\frac{\partial^2 q}{\partial \psi^2} \right)^{-1} \langle \Phi_{ij} \Phi_{im} \Phi_{in} \Phi_{iv} \rangle + 3h \frac{\partial^2 q}{\partial \psi^2} B_{jmnv} \right] A_j^{(1)} A_m^{(1)} A_n^{(1)} = 0, \tag{A19}$$

where $v=1,\ldots,N_i$ and

$$B_{jmnv} = -C_1 \delta_{jm} \delta_{nv} + \sum_{\substack{l=1 \\ l \neq i}}^{\infty} \frac{\sum_{u=1}^{N_l} \langle \Phi_{ij} \Phi_{im} \Phi_{lu} \rangle \langle \Phi_{in} \Phi_{iv} \Phi_{lu} \rangle}{k_l h \coth k_l h - k_i h \coth k_i h}. \tag{A20}$$

In a general case, the system of equations (A19) has a trivial solution, which corresponds to the 1D solution of the original problem, and solution(s) proportional to $\sqrt{|\alpha_2|}$, which correspond to multidimensional solution(s) branching off from the 1D solution. Since $\alpha_1 = 0$, one can set α_2 equal

to 1 or -1 in this case, thus $\varepsilon=\sqrt{2|U-U_i|}$. Perturbations branching off in the considered bifurcation point grow proportionally to $\sqrt{|U-U_i|}$. For $N_i=1$, the above formulas coincide with respective formulas [1] provided T in the formulas [1] is replaced by ψ, Q by qh, y by $1-z/h$, z by y, and k by kh.

The coefficients $A_m^{(1)}$ provide, to a first approximation, a complete description of multidimensional solution(s) in the vicinity of the bifurcation point. In particular, one can calculate the current-voltage characteristics described by these solutions. Expanding the average current density at the cathode surface in the vicinity of a bifurcation point, one gets

$$\langle j\rangle=j_0+\frac{\partial j}{\partial\psi}\left(\varepsilon\langle\psi_1\rangle+\frac{\varepsilon^2}{2}\langle\psi_2\rangle\right)+\frac{\partial j}{\partial U}\left(\varepsilon\alpha_1+\frac{\varepsilon^2}{2}\alpha_2\right)+\frac{\varepsilon^2}{2}\frac{\partial^2 j}{\partial\psi^2}\langle\psi_1^2\rangle+\varepsilon^2\frac{\partial^2 j}{\partial\psi\,\partial U}\langle\psi_1\rangle\alpha_1+\frac{\varepsilon^2}{2}\frac{\partial^2 j}{\partial U^2}\alpha_1^2+\cdots, \tag{A21}$$

where $j_0=j[\psi(U_i),U_i]$ and all the derivatives of the function $j=j(\psi,U)$ are taken at $\psi=\psi(U_i)$, $U=U_i$. Using Eq. (A13) for $p=2$ and Eqs. (A6) and (A14), one finds

$$\langle j\rangle=j_{1\mathrm{D}}+\frac{\varepsilon^2}{2}\left(\frac{\partial^2 j}{\partial\psi^2}-C_1h\frac{\partial j}{\partial\psi}\frac{\partial^2 q}{\partial\psi^2}\right)\sinh^2 k_ih\sum_{m=1}^{N_i}A_m^{(1)2}+\cdots. \tag{A22}$$

Here

$$j_{1\mathrm{D}}=j_0+C_3\alpha_1\varepsilon+\left(C_4\alpha_1^2+\frac{1}{2}C_3\alpha_2\right)\varepsilon^2+\cdots, \tag{A23}$$

where

$$C_3=\frac{\partial j}{\partial U}-C_1h\frac{\partial j}{\partial\psi}\frac{\partial q}{\partial U}, \tag{A24}$$

$$C_4=\frac{1}{2}\frac{\partial^2 j}{\partial U^2}-C_1h\frac{\partial^2 j}{\partial\psi\partial U}\frac{\partial q}{\partial U}-\frac{C_1h}{2}\frac{\partial j}{\partial\psi}\frac{\partial^2 q}{\partial U^2}+(C_1h)^2\frac{\partial j}{\partial\psi}\frac{\partial^2 q}{\partial\psi\partial U}\frac{\partial q}{\partial U}+\frac{(C_1h)^2}{2}\frac{\partial^2 j}{\partial\psi^2}\left(\frac{\partial q}{\partial U}\right)^2-\frac{(C_1h)^3}{2}\frac{\partial j}{\partial\psi}\frac{\partial^2 q}{\partial\psi^2}\left(\frac{\partial q}{\partial U}\right)^2. \tag{A25}$$

Obviously, $j_{1\mathrm{D}}=j_{1\mathrm{D}}(U)$ has the meaning of the current-voltage characteristic described by the 1D solution. To the accuracy to which Eq. (A23) was derived, it can be rewritten as

$$j_{1\mathrm{D}}=j_0+C_3(U-U_i)+C_4(U-U_i)^2+\cdots. \tag{A26}$$

In the first case considered above, when $\varepsilon=U-U_i$, the three terms on the right-hand side of Eq. (A26) must be retained. In the second case, when $\varepsilon=\sqrt{2|U-U_i|}$, the order of magnitude of terms dropped on the right-hand side of Eq. (A22) is $o(|U-U_i|)$, therefore the third term on the right-hand side of Eq. (A26) may be dropped as well.

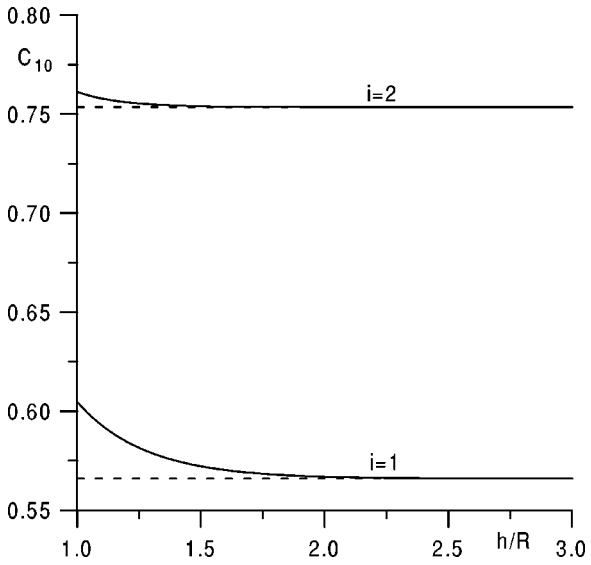

FIG. 9. Coefficient C_{10}.

As an example, we apply the above theory to the case when the cathode is in the form of a circular cylinder, i.e., when G is a circle. The spectrum of the problem (A9) is given by the formula

$$k_{\nu s}R=j'_{\nu,s}, \tag{A27}$$

where $\nu=0,1,2,\ldots$, $s=1,2,3,\ldots$, R is the radius of the cylinder, and $j'_{\nu,s}$ is the sth zero of the derivative of the Bessel function of the first kind of order ν (according to the conventional nomenclature [21], $j'_{0,1}=0$ and $j'_{\nu,1}>0$ for $\nu\geqslant 1$). Suppose that the eigenvalues are numbered in order of their increase:

$$k_0=k_{01}=0,\quad k_1=k_{11}=\frac{j'_{1,1}}{R},\quad k_2=k_{21}=\frac{j'_{2,1}}{R},\quad k_3=k_{02}=\frac{j'_{0,2}}{R},\quad \ldots, \tag{A28}$$

where $j'_{1,1}\approx 1.841$, $j'_{2,1}\approx 3.054$, and $j'_{0,2}\approx 3.832$ [21].

Eigenvalues $k_{\nu s}$ with $\nu=0$ are simple; those with $\nu\geqslant 1$ are doubly degenerated. Orthonormalized eigenfunctions associated with the eigenvalues with $\nu=0$ and to those with $\nu\geqslant 1$ are given by the formulas

$$\Phi_i=\frac{1}{J_0(j'_{0,s})}J_0(k_{0s}r) \tag{A29}$$

and

$$\left.\begin{matrix}\Phi_{i1}\\ \Phi_{i2}\end{matrix}\right\}=\sqrt{\frac{2}{j'^2_{\nu,s}-\nu^2}}\frac{j'_{\nu,s}}{J_\nu(j'_{\nu,s})}J_\nu(k_{\nu s}r)\times\left\{\begin{matrix}\cos\nu\theta\\ \sin\nu\theta\end{matrix}\right., \tag{A30}$$

respectively, where r is the distance from the axis of the cylinder, θ is the azimuthal angle, and $J_\nu(x)$ is the Bessel function of the first kind of order ν.

Consider first a bifurcation point associated with one of the (positive simple) eigenvalues with $\nu=0$, $s=2,3,4,\ldots$.

The system (A17) is reduced to one equation for the only unknown coefficient $A_1^{(1)}$. This equation has a nontrivial root

$$A_1^{(1)}=\frac{C_2C_5}{\sinh k_i h}, \tag{A31}$$

where the numerical coefficient $C_5=-2/\langle\Phi_i^3\rangle$ is given by the formula

$$C_5=-J_0^3(j'_{0,s})\left[\int_0^1 x\,J_0^3(j'_{0,s}x)\,dx\right]^{-1}. \tag{A32}$$

Note that for $i=3$ $(s=2)$, $C_5=2.287$. The asymptotic behavior of the current-voltage characteristic of an axially symmetric solution that branches off at the considered point may be found from Eq. (A22):

$$\langle j\rangle=j_{1D}+\frac{C_5^2}{2}\left(\frac{\partial^2 j}{\partial\psi^2}-C_1h\frac{\partial j}{\partial\psi}\frac{\partial^2 q}{\partial\psi^2}\right)C_2^2(U-U_i)^2+\cdots. \tag{A33}$$

Consider now a bifurcation point associated with one of the (doubly degenerate) eigenvalues with $\nu\geqslant 1$. Since $\langle\Phi_{ij}\Phi_{im}\Phi_{iv}\rangle=0$ for $j,m,v=1$ or 2, one has to employ Eq. (A19). To this end, the quantities $\langle\Phi_{ij}\Phi_{im}\Phi_{in}\Phi_{iv}\rangle$ and B_{jmnv} should be calculated. One finds

$$\langle\Phi_{ij}\Phi_{im}\Phi_{in}\Phi_{iv}\rangle=(\delta_{jm}\delta_{nv}+\delta_{jn}\delta_{mv}+\delta_{jv}\delta_{mn})C_6, \tag{A34}$$

where

$$C_6=\frac{j'^4_{\nu,s}}{(j'^2_{\nu,s}-\nu^2)^2J_\nu^4(j'_{\nu,s})}\int_0^1 x\,J_\nu^4(j'_{\nu,s}x)\,dx. \tag{A35}$$

Note that the numerical coefficient C_6 for $i=1$ $(\nu=1,\ s=1)$ and $i=2$ $(\nu=2,\ s=1)$ equals 0.5840 and 0.6842, respectively.

Calculation of the quantity B_{jmnv} gives

$$B_{jmnv}=\left[-C_1+\frac{R}{h}(C_7-C_8)\right]\delta_{jm}\delta_{nv}+C_8\frac{R}{h}(\delta_{jn}\delta_{mv}+\delta_{jv}\delta_{mn}), \tag{A36}$$

where

$$C_7=\frac{4j'^4_{\nu,s}}{(j'^2_{\nu,s}-\nu^2)^2J_\nu^4(j'_{\nu,s})}\sum_{t=2}^{\infty}\frac{\left[\int_0^1 x\,J_\nu^2(j'_{\nu,s}x)J_0(j'_{0,t}x)dx\right]^2}{J_0^2(j'_{0,t})\left[j'_{0,t}\coth\left(j'_{0,t}\frac{h}{R}\right)-j'_{\nu,s}\coth\left(j'_{\nu,s}\frac{h}{R}\right)\right]}. \tag{A37}$$

$$C_8=\frac{2j'^4_{\nu,s}}{(j'^2_{\nu,s}-\nu^2)^2J_\nu^4(j'_{\nu,s})}\sum_{t=1}^{\infty}\frac{\left[j'_{2\nu,t}\int_0^1 x\,J_\nu^2(j'_{\nu,s}x)J_{2\nu}(j'_{2\nu,t}x)dx\right]^2}{(j'^2_{2\nu,t}-4\nu^2)J_{2\nu}^2(j'_{2\nu,t})\left[j'_{2\nu,t}\coth\left(j'_{2\nu,t}\frac{h}{R}\right)-j'_{\nu,s}\coth\left(j'_{\nu,s}\frac{h}{R}\right)\right]}. \tag{A38}$$

Substituting Eqs. (A34) and (A36) into Eq. (A19), one obtains

$$A_v^{(1)}\left[-\frac{C_9\alpha_2}{\sinh^2 k_i h}+\sum_{m=1}^{2}A_m^{(1)2}\right]=0. \tag{A39}$$

Here $v=1,2$ and

$$C_9=\left(C_1h\frac{\partial^2 q}{\partial\psi^2}\frac{\partial q}{\partial U}-\frac{\partial^2 q}{\partial\psi\,\partial U}\right)\left[C_6\frac{\partial^3 q}{\partial\psi^3}+(C_{10}R-C_1h)\times\left(\frac{\partial^2 q}{\partial\psi^2}\right)^2\right]^{-1}. \tag{A40}$$

The quantity $C_{10}=C_7+C_8$ introduced here is a function of h/R and is shown in Fig. 9 for $i=1$ and $i=2$. The dashed lines represent asymptotic values of this function for large h/R, which are equal to 0.5659 for $i=1$ and 0.7536 for $i=2$. One can see that the dependence of C_{10} on h/R in the range $h\geqslant R$ is in fact rather weak (the variation of C_{10} does not exceed 7% for $i=1$ and 1% for $i=2$). The asymptotic values given above are attained at $h/R\geqslant 2.8$ for $i=1$ and $h/R\geqslant 1.8$ for $i=2$.

For a nontrivial solution, the system (A39) is reduced to one equation, which gives

$$\sum_{m=1}^{2}A_m^{(1)2}=\frac{C_9\alpha_2}{\sinh^2 k_i h}. \tag{A41}$$

Obviously, one must choose $\alpha_2=1$ if $C_9>0$ and $\alpha_2=-1$ if $C_9<0$.

Thus we have been able to determine the sum $A_1^{(1)2}+A_2^{(1)2}$, while the coefficients $A_1^{(1)}$ and $A_2^{(1)}$ separately remain indeterminate. This means that a continuum of solutions of a given amplitude branches off in the point considered. A current-voltage characteristic of any solution of this continuum is the same and is described in the vicinity of the bifurcation point by the formula

$$\langle j\rangle=j_{1D}+\left(\frac{\partial^2 j}{\partial\psi^2}-C_1h\frac{\partial j}{\partial\psi}\frac{\partial^2 q}{\partial\psi^2}\right)C_9(U-U_i)+\cdots. \tag{A42}$$

[1] M. S. Benilov and N. V. Pisannaya, Sov. Phys. Tech. Phys. **33**, 1260 (1988).
[2] M. S. Benilov, Sov. Phys. Tech. Phys. **33**, 1267 (1988).
[3] V. D. Khait, High Temp. **27**, 445 (1989).
[4] W. Thouret, W. Weizel, and P. Günther, Z. Phys. **130**, 621 (1951).
[5] W. Neumann, *The Mechanism of the Thermoemitting Arc Cathode* (Akademie-Verlag, Berlin, 1987).
[6] J. Haidar, J. Phys. D **28**, 2494 (1995).
[7] J. F. Waymouth, J. Light Visual Environ. **6**, 53 (1982).
[8] G. A. Dyuzhev, N. K. Mitrofanov, and S. M. Shkol'nik, Tech. Phys. **42**, 30 (1997).
[9] F. G. Baksht, G. A. Dyuzhev, N. K. Mitrofanov, and S. M. Shkol'nik, Tech. Phys. **42**, 35 (1997).
[10] J. Jenista, J. V. R. Heberlein, and E. Pfender, IEEE Trans. Plasma Sci. **25**, 883 (1997).
[11] E. Fischer, Philips J. Res. **42**, 58 (1987).
[12] W. Weizel and W. Thouret, Z. Phys. **131**, 170 (1952).
[13] B. Y. Moizhes and V. A. Nemchinskii, Sov. Phys. Tech. Phys. **20**, 757 (1975).
[14] M. S. Benilov and A. Marotta, J. Phys. D **28**, 1869 (1995).
[15] M. S. Benilov, Phys. Rev. A **45**, 5901 (1992).
[16] M. S. Benilov and G. V. Naidis, Phys. Rev. E **57**, 2230 (1998).
[17] R. S. Devoto, Phys. Fluids **16**, 616 (1973).
[18] B. Winde, Ann. Phys. (Leipzig) **15**, 57 (1954).
[19] W. Haidinger, Z. Phys. **151**, 106 (1958).
[20] V. S. Vladimirov, *Equations of Mathematical Physics* (Nauka, Moscow, 1976).
[21] *Handbook of Mathematical Functions*, edited by M. Abramowitz and I. A. Stegun (Dover, New York, 1965).